Highlights of the LHC run 1 / Résultats marquants de la première période d'exploitation du GCH

Top quark physics at the LHC

La physique du quark top au GCH

Richard Hawkings

CERN, PH department, CH-1211 Geneva 23, Switzerland

A B S T R A C T

An overview of results on top quark physics from Run 1 of the LHC is presented. The ATLAS and CMS experiments each recorded about 5 fb^{-1} of pp collision data at $\sqrt{s} = 7$ TeV and 20 fb^{-1} at $\sqrt{s} = 8$ TeV, allowing comprehensive studies of t$\bar{\text{t}}$ and single top production, precise measurements of the top mass, and studies of top quark decays. The results are generally in impressive agreement with the predictions of the Standard Model.

© 2015 Académie des sciences. Published by Elsevier Masson SAS. All rights reserved.

R É S U M É

Un panorama des résultats sur la physique du quark top à partir des données du run 1 du LHC est présenté. Les expériences ATLAS et CMS ont enregistré chacune environ 5 fb^{-1} de collisions pp à $\sqrt{s} = 7$ TeV et 20 fb^{-1} à $\sqrt{s} = 8$ TeV. Ces donnée ont permis des études détaillées des modes de production t$\bar{\text{t}}$ et top célibataire, des mesures précises de la masse du quark top et des études des désintégrations du quark top. Les résultats sont en général en très bon accord avec les prédictions du Modèle standard.

© 2015 Académie des sciences. Published by Elsevier Masson SAS. All rights reserved.

1. Introduction

The top quark (t) is the heaviest-known elementary particle, with a mass that is much higher than that of all the other quarks, and close to those of the W, Z and Higgs bosons. It fits naturally into the Standard Model (SM) of particle physics as the up-quark-type partner of the bottom or b quark, completing the three generations of quark flavours, but its large mass of about 173 GeV is about forty times that of the b-quark, a ratio much larger than those seen for the up- and down-type quarks of the first two generations. Its large mass also implies a large partial width for the dominant decay mode t → Wb, corresponding to a very short lifetime of about 10^{-25} s, too short for the top quark to form hadronic bound states with other quarks. The phenomenology of top quark physics is therefore completely different to that of the other quarks, lacking 'top-hadron' spectroscopy, but giving instead the unique opportunity to study the production and decay of a 'bare' quark, at energy scales much larger than those which are typically involved for the other quarks.

The top quark was discovered in 1995 [1] by the CDF and D0 experiments at the Fermilab Tevatron p$\bar{\text{p}}$ collider, which was the only accelerator capable of producing it until the commissioning of the CERN Large Hadron Collider. At the Tevatron
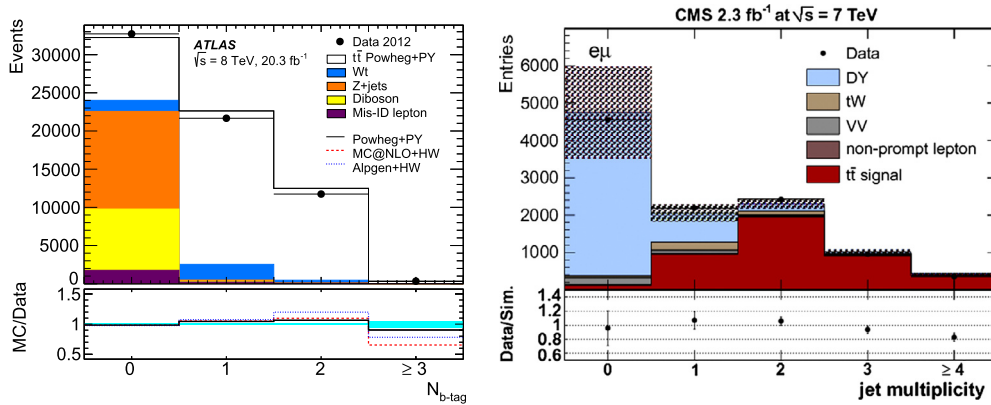
Fig. 1. (Colour online.) Jet multiplicity distributions from dilepton $t\bar{t}$ cross-section analyses: (left) b-tagged jet multiplicity in ATLAS eμ events at $\sqrt{s} = 8$ TeV [5]; (right) jet multiplicity in CMS eμ events passing dilepton and E_T^{miss} requirements before b-tagging selections at $\sqrt{s} = 7$ TeV [12].

centre-of-mass energy ($\sqrt{s}$) of 1.96 TeV, the cross-section for the pair-production $p\bar{p} \rightarrow t\bar{t}$ process is $\sigma_{t\bar{t}} = 7.60 \pm 0.41$ pb [2], corresponding to about 10^5 top–antitop ($t\bar{t}$) pairs for the CDF and D0 experiments in their complete data samples of about 10 fb^{-1} each, before taking event reconstruction and selection efficiencies into account. In pp collisions at the LHC, the $t\bar{t}$ production cross-section is much higher, about 180 pb at $\sqrt{s} = 7$ TeV and 250 pb at $\sqrt{s} = 8$ TeV, giving the two general-purpose LHC experiments, ATLAS and CMS, samples of 6 10^6 $t\bar{t}$ events each before selection cuts from their complete 2011–2012 datasets of 5 fb^{-1} at $\sqrt{s} = 7$ TeV and 20 fb^{-1} at $\sqrt{s} = 8$ TeV. The LHC is thus a true top-quark factory, able to greatly extend the studies performed at the Tevatron, and will dominate the field of top quark physics for the next decade at least.

This article gives a short overview of top physics measurements performed at the $\sqrt{s} = 7$–8 TeV Run 1 of the LHC that were available as of September 2014. It focuses on $t\bar{t}$ production (Sections 2 and 3), single top quark production (Section 4), measurements of the top quark mass (Section 5) and top quark couplings and decay (Section 6). Conclusions and an outlook for Run 2 are given in Section 7. Only a selection of results are given, and the reader is invited to consult the relevant web pages of ATLAS [3] and CMS [4] for further details, including searches for top quarks produced in the decays of hypothesised new particles.

2. Top quark pair production

Top quark pair ($t\bar{t}$) production proceeds through the QCD strong interaction via the subprocesses $gg \rightarrow t\bar{t}$ (about 85% at $\sqrt{s} = 7$ TeV) and $q\bar{q} \rightarrow t\bar{t}$ (15%). It gives rise to various distinctive final states depending on the decay modes of the two W bosons produced in the initial $t \rightarrow Wb$ decays. The dileptonic final state is produced when both W bosons decay to $e\nu$ or $\mu\nu$, giving rise to events with two opposite-sign charged leptons (ee, μμ or eμ), missing transverse momentum (E_T^{miss}) from the undetected neutrinos, and two collimated particle jets from the hadronisation of the b quarks. Additional jets may arise from QCD radiation from the initial-state partons, top quarks or final state quarks. The two leptons, produced with high transverse momentum (p_T) with respect to the directions of the colliding beams, provide the signature used to select the events online. Backgrounds are further rejected by requiring several reconstructed jets, often *tagged* as being likely to have originated from b quarks by making use of the experiments' silicon pixel detectors, which are able to reconstruct the signatures of b-flavoured hadrons decaying several millimetres from the primary interaction point. In this way, pure samples of a few tens of thousands of events have been obtained by both ATLAS and CMS, with residual non-$t\bar{t}$ background contamination of a few percent from the production of W and Z bosons with additional jets, dibosons (in particular WW) and events with a single top quark and a W boson (see Fig. 1). These samples give rise to the most precise measurements of the inclusive production rate or cross-section $\sigma_{t\bar{t}}$, with uncertainties dominated by the knowledge of the integrated luminosity (the total number of pp collisions delivered to the experiments) and the simulation of the kinematic properties of $t\bar{t}$ events, needed to determine the acceptance of the experimental selection cuts.

At $\sqrt{s} = 8$ TeV, the most precise $\sigma_{t\bar{t}}$ measurements come from an ATLAS analysis counting eμ events with one and two b-tagged jets, allowing the cross-section and b-tagged jet selection efficiency to be determined simultaneously [5], and from a CMS analysis of ee, μμ and eμ events with at least two jets, at least one of which has to be b-tagged [6]. The two results are consistent, and have been combined to give a value $\sigma_{t\bar{t}} = 241.4 \pm 8.5$ pb [7], in agreement with the theoretical prediction of $252.9^{+13.3}_{-14.5}$ pb, calculated at full next-to-next-to-leading order (NNLO) accuracy in QCD [8–10], assuming $m_t = 172.5$ GeV. Since $\sigma_{t\bar{t}}$ depends strongly on the centre-of-mass energy $\sqrt{s}$, an additional uncertainty of 4.2 pb arises on the experimental measurement when it is quoted at $\sqrt{s} = 8$ TeV, from the uncertainty in the actual LHC energy compared to the nominal value of $\sqrt{s} = 8$ TeV [11], assuming the dependence of $\sigma_{t\bar{t}}$ on $\sqrt{s}$ to be as predicted by theory.
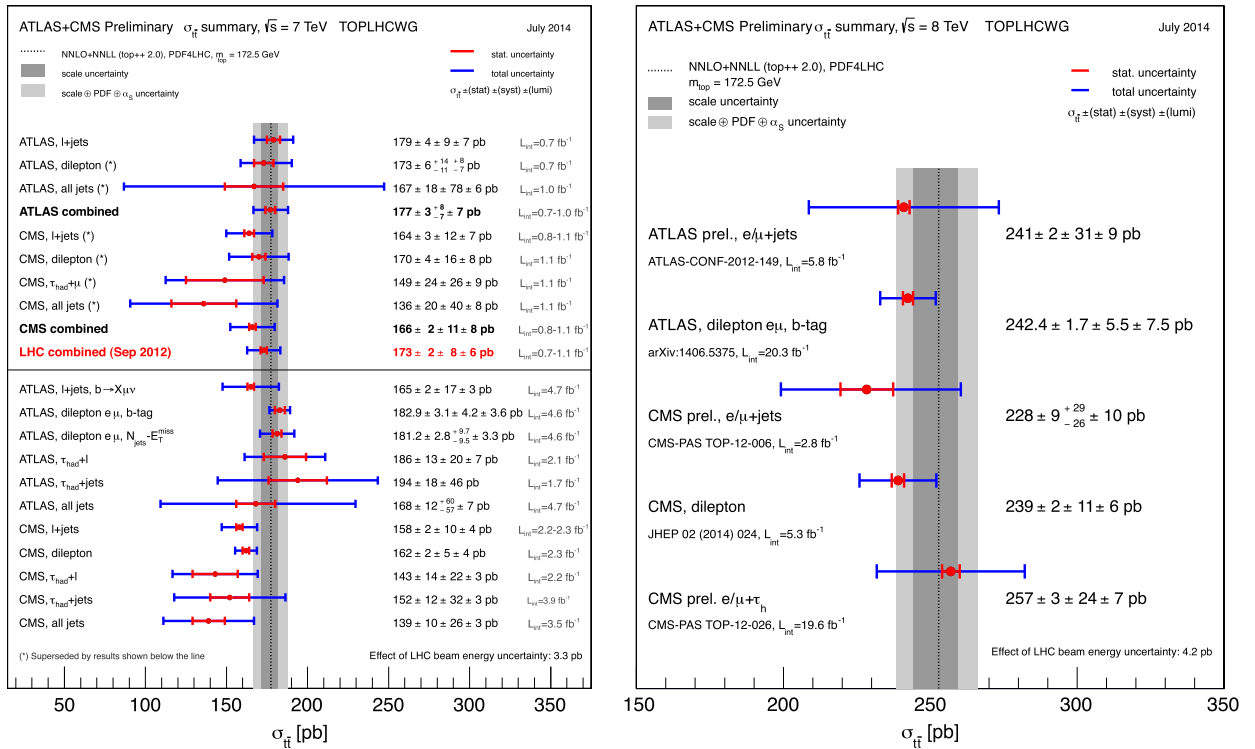
Fig. 2. (Colour online.) Measurements of the $t\bar{t}$ production cross-section at $\sqrt{s} = 7$ TeV (left) and $\sqrt{s} = 8$ TeV (right), compared to the QCD NNLO+NNLL theoretical prediction [9], for an assumed top mass of $m_t = 172.5$ GeV [14]. The left figure includes an early combination of $\sqrt{s} = 7$ TeV measurements; the more precise measurements shown below the line are not included in this combination.

At $\sqrt{s} = 7$ TeV, the ATLAS result from eμ + b-tagged events [5] is in agreement with the theoretical prediction, whilst the CMS dilepton result with a partial dataset of 2.3 fb^{-1} [12] is somewhat lower. These two results disagree by more than two standard deviations, but the final word must wait for an updated CMS analysis of the full 7-TeV dataset.

Only 4.7% of $t\bar{t}$ pairs decay to final states with two electrons or muons. Significantly larger $t\bar{t}$ event samples can be obtained from the 29% of decays to the semileptonic or lepton+jets final state, where the W boson from one top quark decays to eν or $\mu\nu$, and the other to q$\bar{q}$, giving rise to final states with one electron or muon, missing transverse momentum and at least four jets, two from b-quarks. As only one neutrino from W decay is produced, the neutrino four-vector can be inferred by using the measured E_T^{miss} vector and constraining the lepton–neutrino invariant mass to that of the W boson, allowing the kinematics of the two top quarks and the $t\bar{t}$ system to be reconstructed. On the other hand, the non-$t\bar{t}$ backgrounds, from W production accompanied by jets (particularly b-tagged jets), and multijet production with a misidentified lepton, are significantly larger than in dilepton selections, up to 10s of percent depending on the selection cuts used. These samples have also been used to measure $\sigma_{t\bar{t}}$ [13], as shown in Fig. 2, but with lower precision than achieved in dileptons due to the larger backgrounds and more complex topologies involved. W bosons decaying to tau-leptons which subsequently decay hadronically give rise to further classes of events with identified τ candidates. Again, these can be used to measure $\sigma_{t\bar{t}}$, and are of particular interest due to the possibility of top quark decays involving charged Higgs bosons rather than Ws, t $\to$ H$^+$b, which would give rise to an excess of decays involving tau leptons due to the preferential decay of H$^+ \to \tau\nu$. However, no such excesses have been seen [15], and the measurements from all $t\bar{t}$ final states appear consistent.

Finally, in 46% of $t\bar{t}$ events, both W bosons decay hadronically (W $\to$ q$\bar{q}$), giving rise to events with at least six jets, of which two are from b quarks. Such events are very difficult to separate from high-multiplicity QCD multijet production, but $t\bar{t}$ signals can be extracted using b-tagging, event shape and jet p_T requirements. However, the resulting $t\bar{t}$ cross-section measurements [16] suffer from large uncertainties due to the harsh selection cuts and substantial residual backgrounds.

Going beyond the inclusive $t\bar{t}$ cross-section, ATLAS and CMS have provided measurements of differential cross-sections as a function of variables such as the top quark p_T and the p_T, rapidity[1] and invariant mass of the $t\bar{t}$ system. Such measurements require the full reconstruction of the $t\bar{t}$ system kinematics, and an unfolding procedure to correct for acceptance biases and limited detector resolution. The results are typically presented as normalised distributions, to reduce some experimental uncertainties, and the resulting shapes are compared with the predictions of Monte Carlo generators and QCD

---

[1] The rapidity y is related to the direction with respect to the beam line, and defined as $y = \frac{1}{2} \ln \frac{E + p_z}{E - p_z}$ for an object with energy E and momentum p_z in the beam direction.
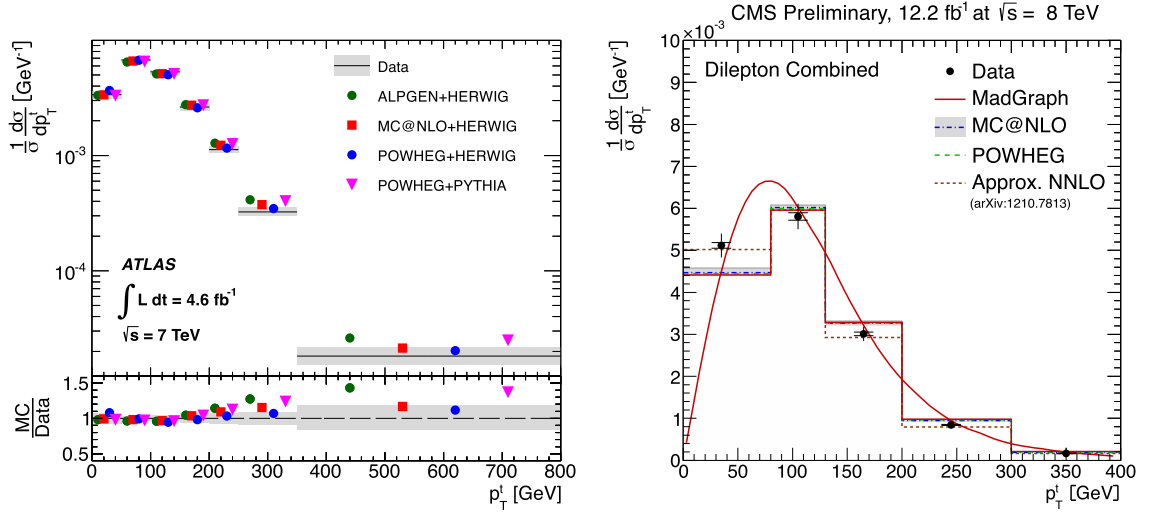
Fig. 3. (Colour online.) Unfolded measurements of the top quark p_T spectrum in the semileptonic channel at $\sqrt{s} = 7$ TeV from ATLAS [17] (left), and the dilepton channel at $\sqrt{s} = 8$ TeV from CMS [20] (right), compared to predictions from various Monte Carlo generators and an approximate NNLO calculation [27].

calculations. Both ATLAS and CMS have published results from the high-statistics semileptonic channel at $\sqrt{s} = 7$ TeV [17, 18], whilst CMS has also released results for dilepton events at $\sqrt{s} = 7$ TeV [18] and preliminary results for semileptonic [19] and dilepton [20] events at $\sqrt{s} = 8$ TeV. Representative results for the top quark p_T distribution are shown in Fig. 3. In general, the top quark kinematics are well-described by both 'multileg' generators such as ALPGEN [21] and MADGRAPH [22], which implement matrix element calculations for $2 \to n$ processes at leading-order, and NLO $t\bar{t}$ generators such as POWHEG [23] and MC@NLO [24], in all cases interfaced to Pythia [25] or Herwig [26] for parton showers and hadronisation. The ATLAS data suggests that all these predictions overestimate the fraction of $t\bar{t}$ production at high top p_T and $t\bar{t}$ invariant mass, whilst the CMS results also suggest a mismodelling at low top p_T, with approximate-NNLO QCD calculations [27] giving a better description than MADGRAPH+PYTHIA. The predictions at high top p_T are sensitive to the distribution of gluons within the proton at high momentum fractions x, which should allow this data to be used in fits to determine proton parton distribution functions [17].

The collaborations have also studied the properties of extra jets from QCD radiation in $t\bar{t}$ events, by using jet multiplicity distributions or by explicitly identifying the jets from the b quarks produced in the top decay using b-tagging [28]. Again, the available Monte Carlo generators generally give a good description of the data, and these studies provide important input in tuning their parameters to reduce modelling uncertainties in different kinematic regions.

3. Top-pair production properties

One of the most intriguing legacy results from the Tevatron is the $t\bar{t}$ forward–backward asymmetry. Analyses of the angular distributions of top quarks and anti-quarks by CDF and D0 indicate that the top quarks (antiquarks) are produced preferentially following the direction of the proton (antiproton) beam, and the size of this asymmetry appears to be slightly larger than expected in the SM [29]. This effect cannot be measured at the LHC, as it collides pp and not p$\bar{\text{p}}$, but an analogous $t\bar{t}$ charge asymmetry A_C can be defined by looking at the difference in absolute rapidity values of the produced top quark and antiquark. The rapidity difference $\Delta|y| = |y_t| - |y_{\bar{t}}|$ is positive when the top quark is produced at a smaller angle to the beam direction (large $|y|$) than the antiquark, and negative otherwise. The asymmetry is defined from event counts N as:

$$A_C = \frac{N(\Delta|y| > 0) - N(\Delta|y| < 0)}{N(\Delta|y| > 0) + N(\Delta|y| < 0)}$$

In the Standard Model, this asymmetry is slightly positive for $t\bar{t}$ pairs produced via $q\bar{q} \to t\bar{t}$, where interference effects generate a correlation between the momentum of the incoming quark and the outgoing top quark, but zero for $gg \to t\bar{t}$. The total resulting asymmetry is small, e.g., an NLO QCD calculation including electroweak corrections gives $A_C = 0.0115 \pm 0.0006$ at $\sqrt{s} = 7$ TeV [30].

Measurements of A_C have been performed by ATLAS and CMS in the semileptonic final state at $\sqrt{s} = 7$ TeV [31]. These analyses fully reconstruct the kinematics of the two top quarks in events with at least four jets, at least one of which is b-tagged. The $\Delta|y|$ distributions are then reconstructed and unfolded to correct for detector effects (see Fig. 4 (left)) to derive the inclusive asymmetry A_C. The $\sqrt{s} = 7$ TeV results from ATLAS and CMS have been combined to measure $A_C = 0.005 \pm 0.007 \pm 0.006$, where the first uncertainty is statistical and the second systematic, dominated by detector and
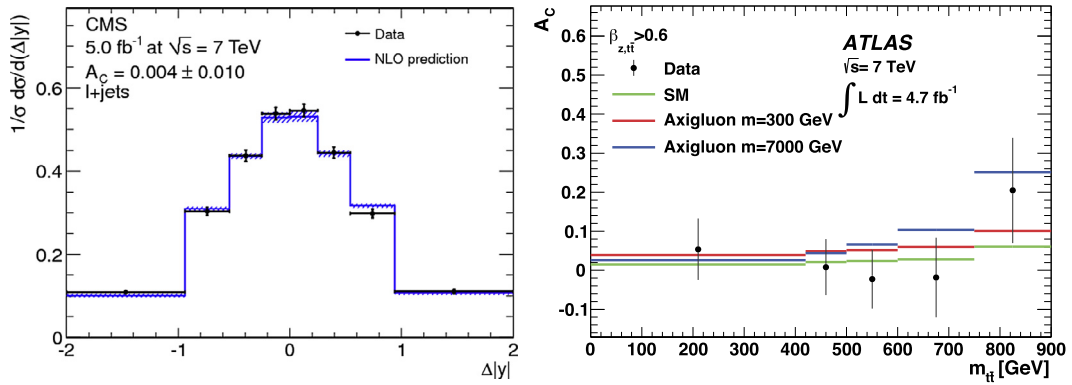
Fig. 4. (Colour online.) Unfolded $\Delta|y|$ distribution from the semileptonic channel at $\sqrt{s} = 7$ TeV in CMS (left), and measurements of A_C as a function of $m_{t\bar{t}}$ at $\sqrt{s} = 7$ TeV from ATLAS, with an additional cut on the velocity of the $t\bar{t}$ system along the beam direction, $\beta > 0.6$, which enhances the fraction of selected $t\bar{t}$ events from $q\bar{q}$ initial states (right) [31].
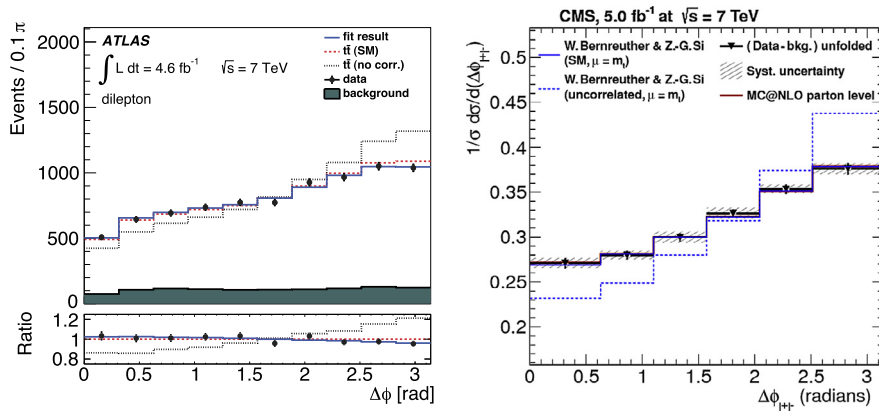

Fig. 5. (Colour online.) Dilepton $\Delta\phi$ distributions showing sensitivity to $t\bar{t}$ spin correlations at $\sqrt{s} = 7$ TeV: reconstructed distribution from ATLAS showing fit to templates with and without spin correlations [35] (left); unfolded distribution from CMS compared to predictions with and without spin correlations [36] (right).

background modelling uncertainties [32]. The result is consistent both with zero and the small asymmetry predicted in the SM, showing no evidence for beyond-Standard-Model (BSM) effects. Measurements have also been performed differentially as a function of various kinematic variables, e.g., $m_{t\bar{t}}$ as shown in Fig. 4 (right), where contributions from BSM physics might be enhanced. The asymmetry A_C has also been measured in dilepton events [33], but the results are of lower precision due to the smaller number of reconstructed events and poorer resolution on the reconstructed $t\bar{t}$ system due to the presence of two neutrinos. Finally, the first results from $\sqrt{s} = 8$ TeV data are becoming available [34]; again, no deviations from SM expectations have been found, strongly constraining some of the models proposed to explain the asymmetry results from the Tevatron experiments.

The short lifetime of the top quark implies that information on its spin at production is transferred to its decay products, where it can be inferred by analysing their angular distributions. In the Standard Model, $t\bar{t}$ production gives rise to top quarks with only a very small amount of polarisation from electroweak effects, but the spins of the quark and anti-quark are expected to be correlated. This correlation is particularly apparent at low invariant mass of the $t\bar{t}$ system, dominated by the fusion of same-helicity gluons, and can be measured using the difference in azimuthal angle $\Delta\phi$ between the two leptons produced in dileptonic $t\bar{t}$ events. Non-zero spin correlations have been seen by both collaborations [35,36], and are well-described by the predictions encoded in the MC@NLO [24] event generator or from dedicated calculations [37], as shown in Fig. 5. Spin correlations have also been observed using more complicated event observables involving products of cosines of decay angles, and jets as well as leptons, and all results are in agreement with SM predictions. Finally, similar techniques can be used to measure the top quark polarisation in $t\bar{t}$ events [36,38] and no polarisation has been seen, again in agreement with expectation.

4. Single top-quark production

As well as the QCD production of $t\bar{t}$ pairs discussed in Section 2, pp collisions at the LHC also give rise to single top quarks via the electroweak interaction, with a total production rate of roughly one half that for $t\bar{t}$. As shown in Fig. 6,
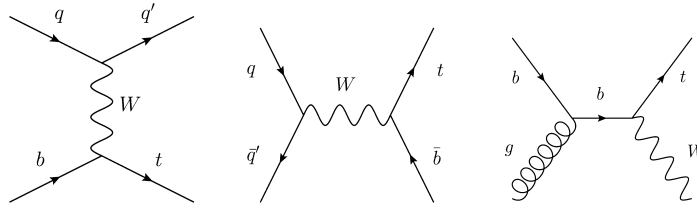
Fig. 6. Leading-order Feynman diagrams for the production of single top quarks in the t-channel (left), s-channel (centre), and for the associated production of a top quark and W boson (tW process) (right).
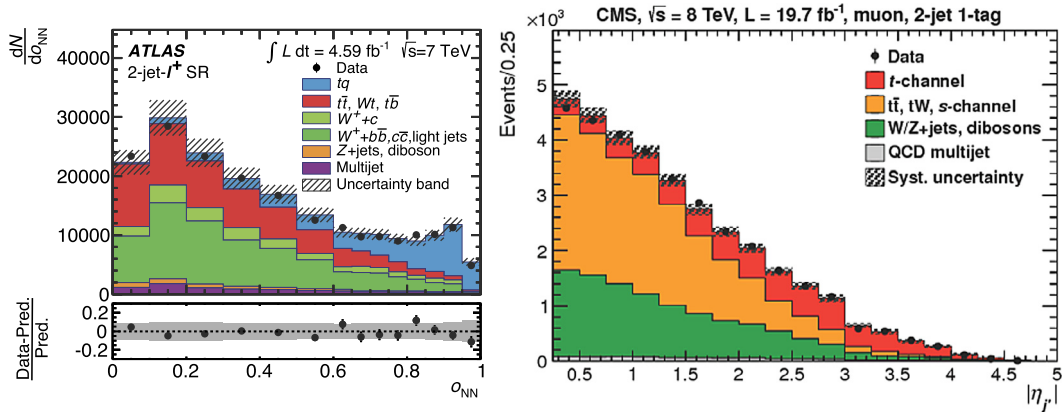

Fig. 7. (Colour online.) Neural network discriminant for events with positively-charged leptons and two jets in the ATLAS $\sqrt{s} = 7$ TeV t-channel single top analysis [42] (left); fitted $|\eta|$ of the untagged jet in events with muons and two jets in the CMS $\sqrt{s} = 8$ TeV t-channel single top analysis [41].

three distinct production processes can be distinguished: the interaction of an initial-state b quark and light quark through W-boson exchange in the t-channel, the interaction of an initial state quark and anti-quark through s-channel W-exchange, and the interaction of a b quark and gluon to produce a top quark and W boson (tW production). At the Tevatron, the first two processes are dominant, and single top production was first observed in 2009 by both CDF and D0 [39]. At the LHC, the t-channel and Wt processes are most important; s-channel production is very small due to the need for a high-momentum antiquark in the initial state, and has not yet been observed [40]. The three processes provide complementary information on the Wtb interaction vertex, whose coupling strength is proportional to the magnitude of the CKM matrix element V_{tb} in the Standard Model.

Single top production in the t-channel gives rise to final states with a lepton and E_T^{miss} from the W boson, a b-tagged jet and an additional high momentum jet from the scattered light quark q′ which usually goes in the forward direction. This final state is difficult to separate cleanly from the major backgrounds of W+jets and $t\bar{t}$ with simple cuts, and multivariate analysis techniques such as boosted decision trees (BDTs) or neural networks are often applied to combine the information from several discriminating variables in each event (see Fig. 7 (left)). CMS has also extracted the signal using a fit to one of the most discriminating individual variables, the rapidity of the light quark jet (Fig. 7 (right)). Both collaborations have measured the production cross-sections for t and $\bar{t}$ quarks separately and combined at both $\sqrt{s} = 7$ TeV and $\sqrt{s} = 8$ TeV, as well as the ratio $\sigma_t/\sigma_{\bar{t}}$, which is sensitive to the differences in PDFs for up- and down-type quarks in the proton [41, 43,42]. The cross-sections have been measured with uncertainties of 9–14%, and are in agreement with approximate-NNLO predictions which have associated uncertainties of around 4% [44]. Assuming the CKM matrix element V_{tb} is much larger than the elements V_{ts} and V_{td} which measure the coupling of top quarks to the lighter s and d quarks, the cross-section results can also be interpreted as measurements of $|V_{tb}|$, e.g., $|V_{tb}| = 0.998 \pm 0.041$ from CMS [41] or $|V_{tb}| = 1.02 \pm 0.07$ from ATLAS [42]. ATLAS has also performed first measurements of differential cross-sections as a function of the p_T and rapidity of the top quark, using a high-purity subsample obtained with a more stringent cut on the neural network output [42] (see Fig. 8 (left)); the resulting distributions are well-described by NLO QCD predictions from the MCFM generator [45].

Associated tW production gives rise to final states with two leptons, E_T^{miss} and one b-tagged jet when both W bosons (including the one from the t → Wb decay) decay leptonically. The predicted tW cross-section at $\sqrt{s} = 8$ TeV is 22.2 ± 1.5 pb [27], an order of magnitude smaller than $t\bar{t}$ leading to a large background from dileptonic $t\bar{t}$ decays when one b-jet from the top decay is missed. Using a BDT (Fig. 8 (right)), the CMS collaboration was able to separate a tW signal from background, measuring $\sigma_{tW} = 23.4 \pm 5.4$ pb with a significance of 6.1 standard deviations [46], thus establishing the existence of this process at about the expected rate. An earlier analysis from ATLAS measured $\sigma_{tW} = 27.2 \pm 5.8$ pb, with a signal significance of 4.1 standard deviations [47]. These analyses can also be used to probe the Wtb vertex and $|V_{tb}|$ in a different kinematic region from t-channel production.
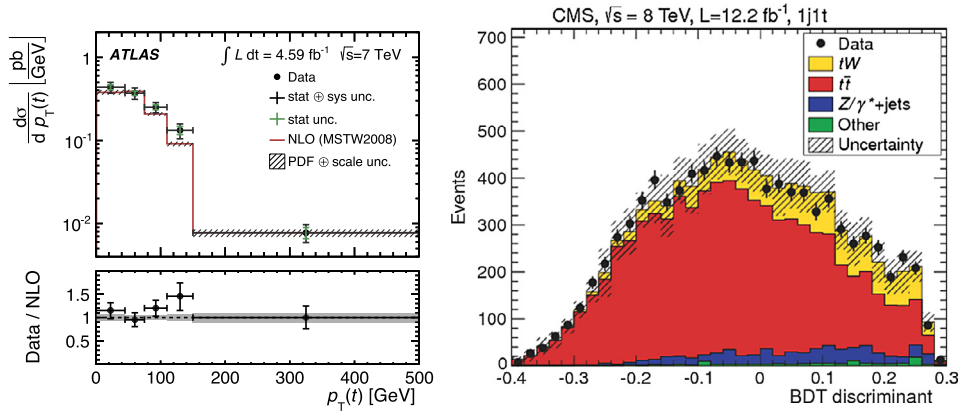
Fig. 8. (Colour online.) Unfolded differential cross-section for t-channel single top production as a function of top quark p_T, measured at $\sqrt{s} = 7$ TeV by ATLAS [42] (left); BDT discriminant for events with two leptons and exactly one jet which is b-tagged in the CMS $\sqrt{s} = 8$ TeV tW associated production analysis [46] (right).
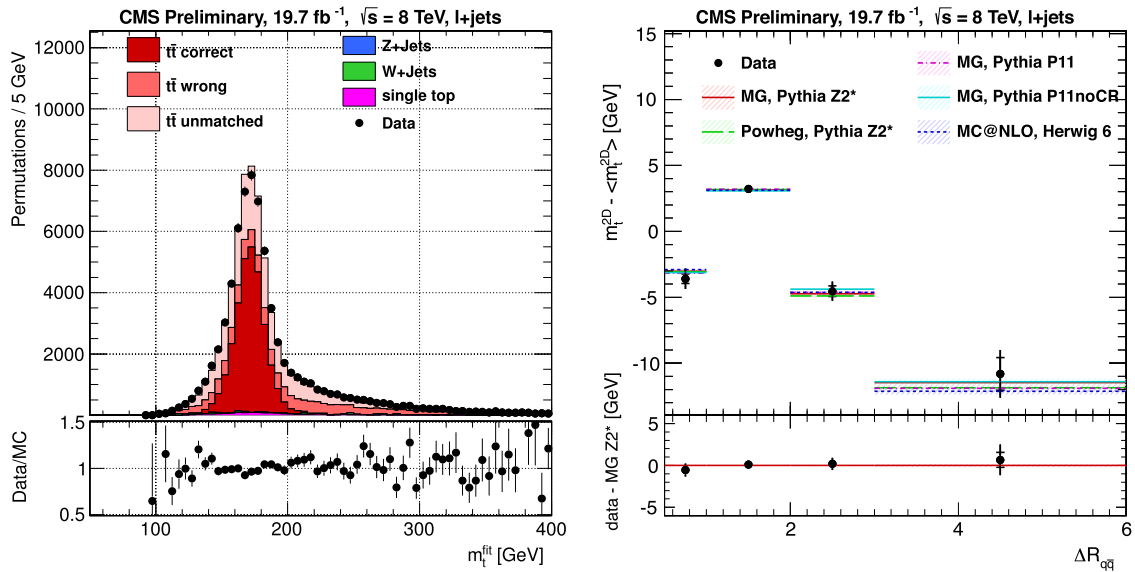

Fig. 9. (Colour online.) Distribution of event-by-event fitted top masses, weighted by the goodness-of-fit of each jet assignment permutation (left) and dependence of the extracted top quark mass on the angular separation $\Delta R_{q\bar{q}}$ between the two light-quark jets from the W boson compared to predictions of various simulation models (right), for the CMS top mass analysis in the semileptonic channel at $\sqrt{s} = 8$ TeV [51].

5. Top mass measurements

The mass of the top quark (m_t) is a fundamental parameter of the Standard Model. The masses of the W and Z bosons are affected by so-called radiative corrections which depend on the quark masses, and which are particularly important for the top quark due to the large value of m_t. Precise measurements of the boson and top quark masses were used to predict the Higgs boson mass, and now that it has been observed, provide an important consistency check for the Standard Model [48]. Depending on the exact value of m_t, the Standard model may or may not have the potential to be valid for energy scales up to the Planck mass, where the effects of gravity become comparable to the other forces [49]. Precise measurements of m_t are therefore key goals of both the Tevatron and LHC physics programmes.

The most precise measurements of m_t come from direct reconstruction of its decay products in the semileptonic channel, typically by using a kinematic fit to reconstruct the most likely top mass for each selected event, taking into account the various possible assignments of the selected lepton and jets to the two top quarks (see Fig. 9 (left)). The dominant experimental uncertainty typically comes from the calibration of the jet energy scale, which directly affects the measured m_t. The CMS analyses [50,51] reduce this with an in-situ jet energy rescaling, requiring the mass of the hadronically-decaying W boson in each event ($W \rightarrow q\bar{q}$) to be consistent with the precisely-known W mass, extracting both the top mass and a jet energy scale factor in a common fit. ATLAS takes this one step further, also using the ratio of the transverse momenta of the jets assigned to the b quark from the top decay and the light quarks from the W decay to give sensitivity to the
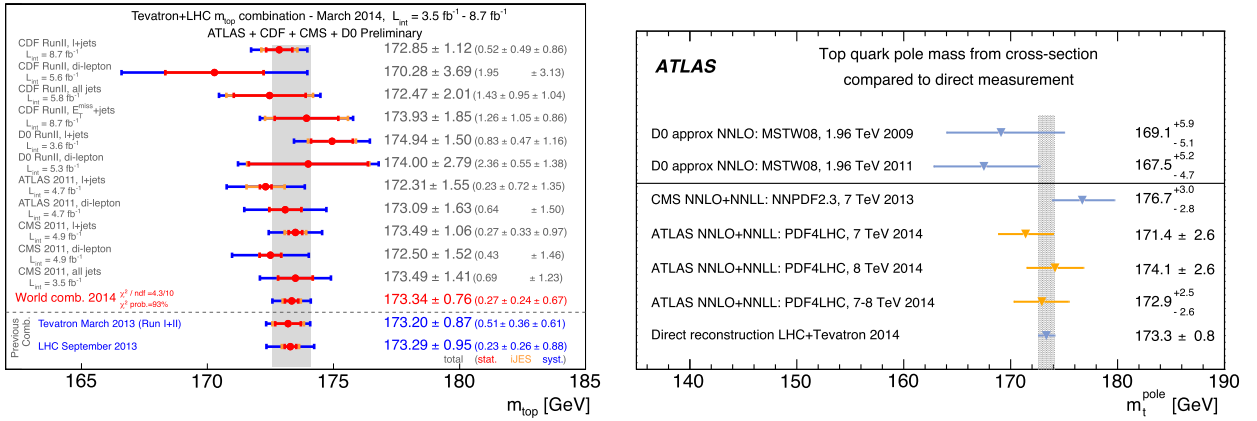
Fig. 10. (Colour online.) Measurements and averages of the top mass via direct reconstruction from Tevatron and LHC experiments [55] (left), and determinations of the top mass from t$\bar{\text{t}}$ cross-section measurements from ATLAS [5], CMS [58] and D0 [59] (right).

energy scale correction for b-jets [52]. Measurements from dileptonic [53] and fully-hadronic [54] events have also been performed, though these have somewhat lower precision.

Fig. 10 (left) shows a compilation of m_t measurements from ATLAS and CMS in various channels compared to measurements from the Tevatron experiments. The results are impressively consistent and have been combined to give a value of $m_t = 173.34 \pm 0.76$ GeV [55], the total uncertainty of 0.44% being dominated by jet calibration and simulation modelling of t$\bar{\text{t}}$ events. Since this combination was performed, two further precise measurements have become available: an analysis in the semileptonic channel at $\sqrt{s} = 8$ TeV from CMS giving 172.04 ± 0.77 GeV [51], and an updated measurement from D0 using semileptonic decays from their full data sample giving 174.98 ± 0.76 GeV [56]. The latter is somewhat higher than the previous world average, and further precise measurements from the other experiments and from the next run of the LHC will be needed to shed light on this discrepancy.

All these measurements determine m_t with respect to the top mass parameter in the associated Monte Carlo simulation, but there are significant theoretical uncertainties of O (1 GeV) in translating this to the top 'pole mass' needed for Standard Model fits and corresponding approximately to the definition of the mass of a free particle [57]. These uncertainties arise because the top quark is a coloured object, so its decay products must exchange colour flow with the rest of the event, potentially modifying their invariant mass. The large LHC data samples are starting to allow the simulation modelling of such effects to be probed, e.g., by measuring how the reconstructed top mass changes as a function of kinematic variables such as the separation $\Delta R_{q\bar{q}}$ between the two light quark jets from the W decay, and comparing the results to Monte Carlo simulations with different models of such 'colour reconnection' effects (see Fig. 9 (right)). Other ways to measure m_t, with different sets of assumptions, are also being explored; e.g., the theoretical predictions for the t$\bar{\text{t}}$ cross-section depend on the assumed top pole mass, allowing the $\sigma_{t\bar{t}}$ measurements described in Section 2 to be interpreted as determinations of m_t, as shown in Fig. 10 (right). These measurements give values consistent with those from direct reconstruction, though the precision is limited to 2–3 GeV, in particular due to the uncertainties on the theoretical cross-section predictions from parton distribution functions and QCD scale uncertainties. Differential measurements in t$\bar{\text{t}} + 1$ jet events also offer a complementary way to measure the pole mass [60], and first experimental results are expected in the near future.

6. Top couplings and rare decays

The large LHC data samples now available provide an opportunity to investigate the couplings of the top quark to the heavy gauge bosons W and Z, via the observation of the associated production processes t$\bar{\text{t}}$W and t$\bar{\text{t}}$Z. The former can be identified in the semileptonic t$\bar{\text{t}}$ decay mode by looking for events with two high p_T same-sign leptons and several jets, some b-tagged. The latter can be identified in both trilepton and four-lepton final states, with two same-flavour (ee or μμ) leptons with invariant mass consistent with a Z-boson decay, and one or two additional leptons consistent with a semileptonic or dileptonic t$\bar{\text{t}}$ final state. The SM t$\bar{\text{t}}$W and t$\bar{\text{t}}$Z cross-sections are small, around 0.2 pb, so only a handful of events are expected. Results from searches at $\sqrt{s} = 8$ TeV from ATLAS [61] and CMS [62] are shown in Fig. 11. Both collaborations see evidence for these processes at about 3σ significance, with rates compatible with the SM expectations, but more data will be required to establish them conclusively. These analyses are a prelude to testing the top–Higgs coupling via observation of the t$\bar{\text{t}}$H process. Only upper limits have been set to date [63], and this is one of the key goals of the next LHC run at 13–14 TeV.

In the Standard Model, the top quark decays 99.8% of the time to Wb, with the remaining 0.2% of decays to Ws and Wd, according to the relative magnitudes of the CKM matrix elements V_{tb}, V_{ts} and V_{td}. This prediction can be tested by counting b-tagged jets in t$\bar{\text{t}}$ events to measure the ratio of branching ratios $R = \mathcal{B}(\text{t} \to \text{Wb})/\mathcal{B}(\text{t} \to \text{Wq})$ where q represents any down-type quark. The most precise Tevatron result, from D0, gave $R = 0.90 \pm 0.04$ [64], significantly smaller than the
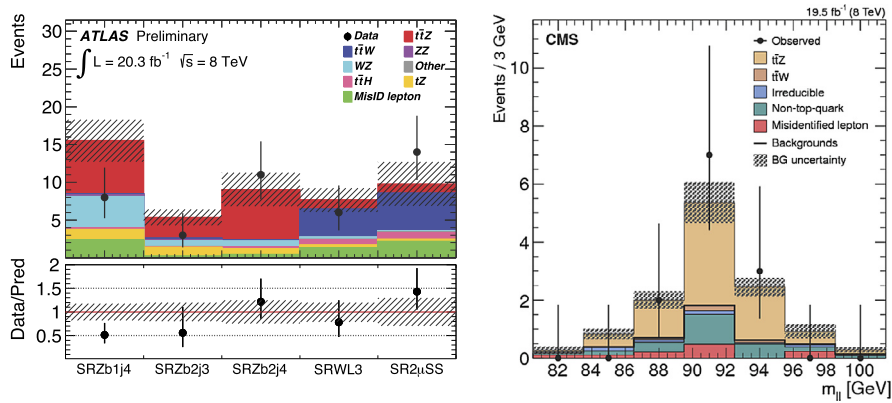
Fig. 11. (Colour online.) Numbers of observed events with three leptons and various numbers of jets, and two same-sign muons, compared with the expected contributions from t̄tZ, t̄tW and various backgrounds in ATLAS $\sqrt{s} = 8$ TeV data [61] (left); dilepton invariant mass distribution in CMS trilepton analysis at $\sqrt{s} = 8$ TeV, highlighting the expected t̄tZ contribution [62] (right).

SM value. However, a recent measurement from CMS in dileptonic t̄t decays using the full $\sqrt{s} = 8$ TeV data sample gives $R = 1.014 \pm 0.032$ [65], in good agreement with the SM prediction. Decays of the form $t \to Zq$ (where q is an up-type quark c or u) involve flavour-changing neutral currents. They can only occur via quantum loops in the SM, leading to a predicted branching fraction of $O(10^{-14})$, but could be as large as 10^{-4}–10^{-5} in some new physics models. Such top quark decays have been probed by looking for events of the form $t\bar{t} \to WbZq$, giving rise to final states with three charged leptons (one from the W, two from the Z) and at least two jets. No signals have been seen, and the most stringent limits come from the complete CMS 7–8 TeV dataset: $\mathcal{B}(t \to Zq) < 0.05\%$ at the 95% confidence level [66].

7. Conclusions and outlook

Thanks to the impressive performance of the accelerator and the ATLAS and CMS detectors, top physics has advanced significantly during Run 1 of the LHC, building on the firm foundations laid at the Tevatron. The dynamics of t̄t production have been studied in detail, and are generally well-described by the state-of-the-art QCD predictions and Monte Carlo event generators, with no hints of BSM physics effects. The tW associated single top production mode has been established, and first differential measurements of single top t channel production have been made. Measurements of the top quark mass have matured quickly, now matching the precision of the legacy Tevatron measurements. The Wtb interaction has been studied in detail, and first measurements of the top quark coupling to W and Z bosons made via the t̄tW and t̄tZ associated production processes. This detailed picture has also allowed a thorough understanding of top quark backgrounds to many new physics searches to be obtained.

At the time of writing, many analyses of the full $\sqrt{s} = 8$ TeV datasets are still in progress, and numerous additional results can be expected in the near future. Beyond that, the 2015–2017 LHC Run 2 at $\sqrt{s} = 13$–14 TeV, with increased integrated luminosity and a t̄t production cross-section 3–4 times that at $\sqrt{s} = 8$ TeV, should give an order-of-magnitude increase in the total number of top quarks recorded for analysis, allowing, e.g., more comprehensive single top quark studies, and the use of alternative methods for the measurement of m_t. So-called 'boosted' topologies, in which the t̄t system is produced with high invariant mass and hence high top quark p_T, will become increasingly important. In these topologies, the decay products of the top quark will no longer be well-separated in the detector, with, e.g., top decays to a single 'fat' jet containing the decay products of both the b quark and W boson, becoming more common. Different analysis techniques such as jet substructure and 'top tagging' will be required to exploit such events, as already explored to some extent in Run 1 [67]. Finally, the larger event samples should allow more detailed studies of top couplings to W and Z, and hopefully a first direct measurement of the top coupling to the Higgs boson.

References

[1] CDF Collaboration, Phys. Rev. Lett. 74 (1995) 2626, arXiv:hep-ex/9503002;
    D0 Collaboration, Phys. Rev. Lett. 74 (1995) 2632, arXiv:hep-ex/9503003.
[2] CDF Collaboration, D0 Collaboration, Phys. Rev. D 89 (2014) 072001, arXiv:1309.7570.
[3] ATLAS top quark physics results, https://twiki.cern.ch/twiki/bin/view/AtlasPublic/TopPublicResults.
[4] CMS top quark physics results, https://twiki.cern.ch/twiki/bin/view/CMSPublic/PhysicsResultsTOP.
[5] ATLAS Collaboration, Eur. Phys. J. C 74 (2014) 3109, arXiv:1406.5375.
[6] CMS Collaboration, J. High Energy Phys. 1402 (2014) 024, arXiv:1312.7582.
[7] ATLAS Collaboration, CMS Collaboration, Combination of ATLAS and CMS top quark pair cross section measurements in the eμ final state using proton–proton collisions at $\sqrt{s} = 8$ TeV, ATLAS-CONF-2014-054, CMS PAS TOP-14-016, https://cds.cern.ch/record/1951322.
[8] M. Beneke, et al., Nucl. Phys. B 855 (2012) 695, arXiv:1109.1536;
    M. Cacciari, et al., Phys. Lett. B 710 (2012) 612, arXiv:1111.5869;

P. Bärnreuther, et al., Phys. Rev. Lett. 109 (2012) 132001, arXiv:1204.5201;
M. Czakon, A. Mitov, J. High Energy Phys. 1212 (2012) 054, arXiv:1207.0236;
M. Czakon, A. Mitov, J. High Energy Phys. 1301 (2013) 080, arXiv:1210.6832;
M. Czakon, P. Fiedler, A. Mitov, Phys. Rev. Lett. 110 (2013) 252004, arXiv:1303.6254.
[9] M. Czakon, A. Mitov, Comput. Phys. Commun. 185 (2014) 2930, arXiv:1112.5675.
[10] M. Beneke, et al., J. High Energy Phys. 1207 (2012) 194, arXiv:1206.2454.
[11] J. Wenninger, Energy calibration of the LHC beams at 4 TeV, CERN-ATS-2013-40, http://cds.cern.ch/record/1546734.
[12] CMS Collaboration, J. High Energy Phys. 1211 (2012) 067, arXiv:1208.2671.
[13] ATLAS Collaboration, ATLAS-CONF-2011-121, http://cdsweb.cern.ch/record/1376413;
CMS Collaboration, Phys. Lett. B 720 (2013) 83, arXiv:1212.6682;
CMS Collaboration, CMS PAS TOP-12-006, http://cdsweb.cern.ch/record/1461939;
ATLAS Collaboration, ATLAS-CONF-2012-149, http://cdsweb.cern.ch/record/1493488.
[14] LHC Top Physics Working Group, https://twiki.cern.ch/twiki/bin/view/LHCPhysics/TopLHCWG.
[15] CMS Collaboration, J. High Energy Phys. 1207 (2012) 143, arXiv:1205.5736;
ATLAS Collaboration, ATLAS-CONF-2013-090, http://cdsweb.cern.ch/record/1595533.
[16] ATLAS Collaboration, ATLAS-CONF-2012-031, http://cdsweb.cern.ch/record/1432196;
CMS Collaboration, J. High Energy Phys. 1305 (2013) 065, arXiv:1302.0508.
[17] ATLAS Collaboration, Phys. Rev. D 90 (2014) 072004, arXiv:1407.0371.
[18] CMS Collaboration, Eur. Phys. J. C 73 (2013) 2339, arXiv:1211.2220.
[19] CMS Collaboration, CMS PAS TOP-12-027, http://cdsweb.cern.ch/record/1523611.
[20] CMS Collaboration, CMS PAS TOP-12-028, http://cdsweb.cern.ch/record/1523664.
[21] M.L. Mangano, et al., J. High Energy Phys. 0307 (2003) 001, arXiv:hep-ph/0206293.
[22] J. Alwall, et al., arXiv:1106.0522.
[23] P. Nason, J. High Energy Phys. 0411 (2004) 040, arXiv:hep-ph/0409146;
S. Frixione, P. Nason, C. Oleari, J. High Energy Phys. 0711 (2007) 070, arXiv:0709.2092.
[24] S. Frixione, B. Webber, J. High Energy Phys. 0206 (2002) 029, arXiv:hep-ph/0204244.
[25] S. Mrenna, T. Sjöstrand, P. Skands, J. High Energy Phys. 05 (2006) 026, arXiv:hep-ph/0603175.
[26] G. Corcella, et al., J. High Energy Phys. 0101 (2011) 010, arXiv:hep-ph/0011363.
[27] N. Kidonakis, Phys. Part. Nucl. 45 (2014) 714, arXiv:1210.7813.
[28] ATLAS Collaboration, Eur. Phys. J. C 72 (2012) 2043, arXiv:1203.5015;
CMS Collaboration, Eur. Phys. J. C 74 (2014) 3014, arXiv:1404.3171;
ATLAS Collaboration, J. High Energy Phys. 1501 (2015) 020, arXiv:1407.0891.
[29] CDF Collaboration, Phys. Rev. D 87 (2013) 092002, arXiv:1211.1003;
CDF Collaboration, Phys. Rev. D 88 (2013) 072003, arXiv:1308.1120;
CDF Collaboration, Phys. Rev. Lett. 113 (2014) 042001, arXiv:1004.3698;
D0 Collaboration, Phys. Rev. D 90 (2014) 072001, arXiv:1403.1294;
D0 Collaboration, Phys. Rev. D 90 (2014) 072011, arXiv:1405.0421.
[30] J.H. Kühn, G. Rodrigo, J. High Energy Phys. 1201 (2012) 063, arXiv:1109.6830.
[31] CMS Collaboration, Phys. Lett. B 717 (2012) 129, arXiv:1207.0065;
ATLAS Collaboration, J. High Energy Phys. 1402 (2014) 107, arXiv:1311.6724.
[32] ATLAS Collaboration, CMS Collaboration, Combination of ATLAS and CMS $t\bar{t}$ charge asymmetry measurements using LHC proton–proton collisions at $\sqrt{s} = 7$ TeV, ATLAS-CONF-2014-012, CMS PAS TOP-14-006, https://cds.cern.ch/record/1670535.
[33] CMS Collaboration, J. High Energy Phys. 1404 (2014) 191, arXiv:1402.3803.
[34] CMS Collaboration, CMS PAS TOP-12-033, http://cdsweb.cern.ch/record/1600839.
[35] ATLAS Collaboration, Phys. Rev. D 90 (2014) 112016, arXiv:1407.4314.
[36] CMS Collaboration, Phys. Rev. Lett. 112 (2014) 182001, arXiv:1311.3924.
[37] W. Bernreuther, Z.-G. Si, Phys. Lett. B 725 (2013) 115, arXiv:1305.2066.
[38] ATLAS Collaboration, Phys. Rev. Lett. 111 (2013) 232002, arXiv:1307.6511.
[39] D0 Collaboration, Phys. Rev. Lett. 103 (2009) 092001, arXiv:0903.0850;
CDF Collaboration, Phys. Rev. Lett. 103 (2009) 092002, arXiv:0903.0885.
[40] CMS Collaboration, CMS PAS TOP-13-009, http://cdsweb.cern.ch/record/1633190.
[41] CMS Collaboration, J. High Energy Phys. 1212 (2012) 035, arXiv:1209.4533;
CMS Collaboration, J. High Energy Phys. 1406 (2014) 090, arXiv:1403.7366.
[42] ATLAS Collaboration, Phys. Rev. D 90 (2014) 112006, arXiv:1406.7844.
[43] ATLAS Collaboration, ATLAS-CONF-2014-007, http://cdsweb.cern.ch/record/1668960.
[44] N. Kidonakis, Phys. Rev. D 83 (2011) 091503, arXiv:1103.2792.
[45] J.M. Campbell, R.K. Ellis, Nucl. Phys. Proc. Suppl. 205 (2010) 10, arXiv:1007.3492.
[46] CMS Collaboration, Phys. Rev. Lett. 112 (2014) 231802, arXiv:1401.2942.
[47] ATLAS Collaboration, ATLAS-CONF-2013-100, http://cdsweb.cern.ch/record/1600799.
[48] M. Baak, et al., Eur. Phys. J. C 72 (2012) 2205, arXiv:1209.2716.
[49] G. Degrassi, et al., J. High Energy Phys. 1208 (2012) 098, arXiv:1205.6497;
S. Alekhin, et al., Phys. Lett. B 716 (2012) 214, arXiv:1207.0980.
[50] CMS Collaboration, J. High Energy Phys. 1212 (2012) 105, arXiv:1209.2319.
[51] CMS Collaboration, CMS PAS TOP-14-001, http://cdsweb.cern.ch/record/1690093.
[52] ATLAS Collaboration, ATLAS-CONF-2013-046, http://cdsweb.cern.ch/record/1547327.
[53] CMS Collaboration, Eur. Phys. J. C 72 (2012) 2202, arXiv:1209.2393;
ATLAS Collaboration, ATLAS-CONF-2013-077, http://cdsweb.cern.ch/record/1562935.
[54] CMS Collaboration, Eur. Phys. J. C 74 (2014) 2758, arXiv:1307.4617;
ATLAS Collaboration, Eur. Phys. J. C 75 (2015) 158, arXiv:1409.0832.
[55] ATLAS Collaboration, CDF Collaboration, CMS Collaboration, D0 Collaboration, arXiv:1403.4427.
[56] D0 Collaboration, Phys. Rev. Lett. 113 (2014) 032002, arXiv:1405.1756.
[57] A. Buckley, et al., Phys. Rep. 504 (2011) 145, arXiv:1101.2599;
S. Moch, et al., arXiv:1405.4781.
[58] CMS Collaboration, Phys. Lett. B 728 (2014) 496, arXiv:1307.1907v3.

[59] D0 Collaboration (V. Abazov et al.), Phys. Rev. D 80 (2009) 071102, arXiv:0903.5525;
     D0 Collaboration (V. Abazov et al.), Phys. Lett. B 703 (2011) 422, arXiv:1104.2887.
[60] S. Alioli, et al., Eur. Phys. J. C 73 (2013) 2438, arXiv:1303.6415.
[61] ATLAS Collaboration, ATLAS-CONF-2014-038, http://cdsweb.cern.ch/record/1735215.
[62] CMS Collaboration, Eur. Phys. J. C 74 (2014) 3060, arXiv:1406.7830.
[63] ATLAS Collaboration, ATLAS-CONF-2014-011, http://cdsweb.cern.ch/record/1670532;
     ATLAS Collaboration, ATLAS-CONF-2014-43, http://cdsweb.cern.ch/record/1740974;
     CMS Collaboration, J. High Energy Phys. 1409 (2014) 087, arXiv:1408.1682.
[64] D0 Collaboration, Phys. Rev. Lett. 107 (2011) 121802, arXiv:1106.5436.
[65] CMS Collaboration, Phys. Lett. B 736 (2014) 33, arXiv:1404.2292.
[66] CMS Collaboration, Phys. Rev. Lett. 112 (2014) 171802, arXiv:1312.4194.
[67] ATLAS Collaboration, J. High Energy Phys. 1301 (2013) 116, arXiv:1211.2202;
     ATLAS Collaboration, Phys. Rev. D 88 (2013) 012004, arXiv:1305.2756;
     CMS Collaboration, Phys. Rev. Lett. 111 (2013) 211804, arXiv:1309.2030.